On the current sheet model with κ distribution

Peter H. Yoon*
IPST, University of Maryland, College Park, MD 20742-2431

Anthony T. Y. Lui†
APL, Johns Hopkins University, Laurel, MD 20723-6099

Robert B. Sheldon‡
MSFC, Huntsville, AL
(Dated: June 13, 2006)

The present paper (re)derives current sheet equilibrium solutions on the basis of the so-called κ distribution functions for the particles. The purpose of the present paper is to remedy a shortcoming in a recent paper [W.-Z. Fu and L.-N. Hau, Phys. Plasmas **12**, 070701 (2005)], where the authors first formulated the equilibrium current sheet model with the κ distribution. Although mathematically correct, their model contains a peculiarly unphysical feature in that the global temperature profile diverges in the asymptotic regime. The present paper shows that such an unphysical characteristics can be rectified if one assumes a finite stationary background population of the particles. We further extend the analysis by considering a current sheet model where the electron current is embedded within a thicker ion current layer, and where there exists a weak electrostatic potential drop across the current sheet.

I. INTRODUCTION

Space plasmas are found in many diverse parameter regimes. Transition between one plasma regime to the next often occurs in a narrow layer where strong currents flow. The boundary layer thus forms a current sheet through which mass, momentum, and energy can be communicated between these plasma regimes. In addition, energy transformation from fields to particles or *vice versa* can take place in these current sheets. For instance, in magnetospheric research, prominent features such as bow shock, magnetopause, and cross-tail current are examples of these current sheets found in every planetary magnetosphere and magnetized moon so far explored [1, 2]. Of high interest are dynamic processes such as magnetic reconnection and current disruption that reside in these current sheets [3–10]. As a result of the particle interaction with the turbulence driven by these dynamic processes, particle populations in these current sheets deviate from thermal equilibrium, resulting in their velocity distribution, departing from the well-known Maxwellian (or gaussian) distribution (e.g, see Ref. [11]).

One of the most commonly employed models of the current sheet equilibria is the classic Harris solution [12]. A fundamental assumption in the Harris solution is that the particle distribution is specified by a gaussian velocity distribution function. In space environment, however, purely gaussian distributions of particles are almost never observed, as mentioned above. Instead, particle distributions feature extended energetic tail population, often modeled by the so-called κ distribution function [13]. Recently, the κ distribution has attracted much attention, not simply as a convenient mathematical analytical model to fit the data, but as a potentially legitimate theoretical model representing an equilibrium solution of an alternative thermodynamic state. The recent trend was initiated by the work of Tsallis [14], who proposed an alternative definition of the entropy. The thermodynamical theory that relies on the Tsallis entropy came to be known as the non-extensive thermostatics [15–19], and according to such a theory, the equilibrium state of a system governed by the non-extensive entropy law corresponds to the κ distribution. In contrast, the textbook thermostatics theory based upon the classic Boltzmann-Gibbs definition of the entropy results in the gaussian model as the equilibrium solution.

In a recent paper Fu and Hau [20] obtained a one-dimensional current sheet equilibrium solution on the basis of the κ distribution, which is a direct generalization of the Harris equilibrium. We shall present a brief overview of their solution in the next section, but we hasten to point out that although their model better represents the real situation in nature (and their solution is certainly mathematically correct), a peculiar feature of the κ-distribution model of the current sheet is that the effective kinetic temperature monotonically increases as one moves away from the neutral sheet, which needlessly to say, is apparently unphysical.

The purpose of the present discussion is to rectify the unphysical temperature profile associated with the curren sheet model proposed in Ref. [20]. We also propose further generalization of the model in Ref. [20], in which the current sheet can possess a weak electrostatic potential. The weakly charged current sheet model in the context of the gaussian distribution was first formulated in Ref. [21]. The model to be discussed later differs from that of Ref. [21] in that the particle distribution is the κ model instead of the gaussian.

II. CURRENT SHEET EQUILIBRIA WITH κ DISTRIBUTION

In the present analysis, we assume that average plasma number density varies along the z axis. The ambient magnetic field is directed along the x axis (hence, we only need to be concerned with the y component vector potential), and the electric field vector is directed along the z axis. The non-trivial invariants of the equilibrium Vlasov equation are the canonical momentum and total Hamiltonian, given respectively by

$$\begin{aligned} P_{yj} &= m_j v_y + \frac{e_j A_y}{c}, \\ H_j &= \frac{m_j v^2}{2} + e_j \phi, \end{aligned} \tag{1}$$

where m_j and e_j are the mass and unit charge for particle species labeled j ($= i, e$ for protons and electrons, respectively), A_y and ϕ are vector and scalar potentials, and c is the speed of light *in vacuo*.

Fu and Hau [20] constructed a single component equilibrium particle distribution for each species, on the basis of the κ distribution whose arguments are the above invariants. However, as we shall see, such a construction leads to an unphysical result where the effective particle temperature becomes infinite in the asymptotic regime ($z \to \infty$). To avoid such an outcome we thus consider a stationary background population of particles in addition to the drifting components which carry the current and are therefore responsible for maintaining the magnetic field reversal profile. We assume a simple gaussian distribution for the background population. The particle distribution is therefore given by

$$\begin{aligned} F_j(z, \mathbf{v}) &= \frac{\delta\, n_0}{\pi^{3/2}\,(2\theta_{j0}/m_j)^{3/2}}\, \exp\left(-\frac{H_j}{\theta_{j0}}\right) \\ &+ \frac{(1-\delta)\, n_0}{\pi^{3/2}\,(2\theta_j/m_j)^{3/2}} \frac{\Gamma(\kappa+1)}{\kappa^{3/2}\,\Gamma(\kappa-1/2)} \\ &\times \left(1 + \frac{H_j - V_j P_{yj} + m_j V_j^2/2}{\kappa\,\theta_j}\right)^{-\kappa-1}. \end{aligned} \tag{2}$$

The following velocity moments of the above distribution function are of particular interest:

$$\begin{aligned} n_j &= \int d\mathbf{v}\; F_j = \delta\, n_0\, \exp\left(-\frac{e_j\phi}{\theta_{j0}}\right), \\ &+ (1-\delta)\, n_0 \left(1 + \frac{e_j\phi}{\kappa\,\theta_j} - \frac{e_j V_j A_y}{\kappa\, c\,\theta_j}\right)^{-\kappa+1/2}, \\ n_j \langle v_y \rangle_j &= \int d\mathbf{v}\; v_y\, F_j = (1-\delta)\, n_0 V_j \\ &\times \left(1 + \frac{e_j\phi}{\kappa\,\theta_j} - \frac{e_j V_j A_y}{\kappa\, c\,\theta_j}\right)^{-\kappa+1/2}, \\ n_j T_j &= \frac{m_j}{3} \int d\mathbf{v}\; (\mathbf{v} - \langle \mathbf{v} \rangle)^2\; F_j \\ &= \delta\, n_0 \theta_{j0}\, \exp\left(-\frac{e_j\phi}{\theta_{j0}}\right) + (1-\delta)\, n_0 \theta_j \\ &\times \frac{\kappa}{\kappa - 3/2} \left(1 + \frac{e_j\phi}{\kappa\,\theta_j} - \frac{e_j V_j A_y}{\kappa\, c\,\theta_j}\right)^{-\kappa+3/2}. \end{aligned} \tag{3}$$

In Eqs. (2) and (3), n_j defines the average number density; $\langle v_j \rangle_j$ signifies the average particle flow velocity profile along the cross-field direction; and the quantity T_j represents the effective kinetic temperature of the system, which is related to the parameter θ_{j0} and θ_j. Without the background population, that is, when $\delta = 0$, it will be shown later that $T_j \to \infty$ as $z^2 \to \infty$.

Making use of the above velocity moments, one can easily compute the electric charge density, $\rho = \sum_j e_j n_j$, and the cross-field current density, $J_y = \sum_j e_j n_j \langle v_y \rangle$. Inserting ρ and J_y to the quasi-neutrality condition $n_i \approx n_e$ and the y component of the Ampere's law, one obtains

$$\begin{aligned} 0 &= \delta \sum_j e_j \exp\left(-\frac{e_j\phi}{\theta_{j0}}\right) \\ &+ (1-\delta) \sum_j e_j \left(1 + \frac{e_j\phi}{\kappa\,\theta_j} - \frac{e_j V_j A_y}{\kappa\, c\,\theta_j}\right)^{-\kappa+1/2}, \end{aligned} \tag{4}$$

$$\begin{aligned} \frac{d^2 A_y}{dz^2} &= -\frac{4\pi}{c}\,(1-\delta)\, n_0 \sum_j e_j V_j \\ &\times \left(1 + \frac{e_j\phi}{\kappa\,\theta_j} - \frac{e_j V_j A_y}{\kappa\, c\,\theta_j}\right)^{-\kappa+1/2}. \end{aligned} \tag{5}$$

Equations and (4) and (5) reduce to those considered in Ref. [20] if we set $\delta = 0$, and trivially satisfy Eq. (4) by making the choice $V_i/\theta_i = -V_e/\theta_e$ and by assuming $\phi = 0$. By contrast, we shall be interested in the finite δ within the range $0 < \delta < 1$. A further generalization of Ref. [20] is to permit V_i/θ_i to be generally different from $-V_e/\theta_e$ [21]:

$$\frac{V_i}{\theta_i} \neq -\frac{V_e}{\theta_e}. \tag{6}$$

Once we invoke Eq. (6), it is no longer possible to ignore Eq. (4), but instead, one must solve ϕ from Eq. (4). The exact analytical solution is not forthcoming, but if we are interested in a weakly charge current sheet, satisfying the condition

$$\frac{e\phi}{\theta_i} \ll 1, \tag{7}$$

then the electrostatic potential can be solved in an approxmate manner:

$$\begin{aligned} \Psi \equiv \frac{e\phi}{T_i} &= \left\{ \frac{\delta}{1-\delta} \frac{\theta_{i0} + \theta_{e0}}{\theta_{e0}} + \frac{\kappa - 1/2}{\kappa} \right. \\ &\times \left. \left[\left(1 + \frac{2Y}{\kappa}\right)^{-\kappa-1/2} + \frac{1}{\tau} \left(1 + \frac{2Y}{\kappa U \tau}\right)^{-\kappa-1/2} \right] \right\}^{-1} \end{aligned}$$

$$\times \left[\left(1+\frac{2Y}{\kappa}\right)^{-\kappa+1/2} - \left(1+\frac{2Y}{\kappa U\tau}\right)^{-\kappa+1/2}\right], \quad (8)$$

where

$$\begin{aligned} \tau &= \frac{\theta_e}{\theta_i}, \\ U &= \frac{V_i}{|V_e|}, \\ Y &= -\frac{eV_iA_y}{2c\theta_i}. \end{aligned} \quad (9)$$

Having obtain the electrostatic potential Ψ in terms of the vector potential Y, we now insert Ψ to Eq. (5), which is expressed in dimensionless form as

$$\begin{aligned} \frac{d^2Y}{dZ^2} &= \frac{1}{1+\tau}\left[\left(1+\frac{\Psi}{\kappa}+\frac{2Y}{\kappa}\right)^{-\kappa+1/2}\right. \\ &+ \left.\frac{1}{U}\left(1-\frac{\Psi}{\kappa\tau}+\frac{2Y}{\kappa U\tau}\right)^{-\kappa+1/2}\right], \end{aligned} \quad (10)$$

where

$$\begin{aligned} Z &= \frac{z}{L}, \\ L &= \frac{c\theta_i}{eV_i\sqrt{2\pi(1-\delta)\,n_0\,(\theta_i+\theta_e)}}. \end{aligned} \quad (11)$$

Equation (10) reduces to the simple equation derived in Ref. [20],

$$\frac{d^2Y}{dZ^2} = \left(1+\frac{2Y}{\kappa}\right)^{-\kappa+1/2}, \quad (12)$$

if we consider $U = 1/\tau$ and $\Psi = 0$. This equation is a particular example of a generic class of equations

$$\frac{d^2w}{dx^2} = w^m,$$

which has a formal analytic solution in parametric form [20, 22],

$$x = \pm\int\left(\frac{2}{m+1}\,w^{m+1}+C_1\right)^{-1/2} dw + C_2,$$

if $m \neq -1$ and

$$x = \pm\int\left(2\ln|w|+C_1\right)^{-1/2} dw + C_2,$$

if $m = -1$. Reference [20] employs the above parametric solution. However, since the w integral must be performed by numerical means, the formal analytic solution of Eq. (12) in parametric form considered in Ref. [20] offers no intrinsic advantage over the direct numerical solution of the original differential equation (12). Besides, when $U\tau \neq 1$ and $\Psi \neq 0$ in general, the coupled equations of interest to us, namely, (8) and (10), do not even enjoy a formal solution. Therefore, in the subsequent section, we solve Eqs. (8) and (10) by a direct numerical approach.

In terms of the normalized variables (9) and (11), the velocity moments (3) can be expressed as

$$\begin{aligned} \frac{n_i}{n_0} &= \delta\,(1-\Psi) + \frac{1-\delta}{(1+\Psi/\kappa+2Y/\kappa)^{\kappa-1/2}}, \\ \frac{n_e}{n_0} &= \delta\left(1+\frac{\Psi}{\tau}\right) + \frac{1-\delta}{(1-\Psi/\kappa\tau+2Y/\kappa U\tau)^{\kappa-1/2}}, \\ \frac{n_i}{n_0}\frac{\langle v_y\rangle_i}{V_i} &= \frac{1-\delta}{(1+\Psi/\kappa+2Y/\kappa)^{\kappa-1/2}}, \\ \frac{n_e}{n_0}\frac{\langle v_y\rangle_e}{V_i} &= -\frac{1}{U}\frac{1-\delta}{(1-\Psi/\kappa\tau+2Y/\kappa U\tau)^{\kappa-1/2}}, \\ \frac{n_i}{n_0}\frac{T_i}{\theta_i} &= \delta\,\frac{\theta_{i0}}{\theta_i}\,(1-\Psi) \\ &+ \frac{\kappa}{\kappa-3/2}\frac{1-\delta}{(1+\Psi/\kappa+2Y/\kappa)^{\kappa-3/2}}, \\ \frac{n_e}{n_0}\frac{T_e}{\theta_i} &= \delta\,\frac{\theta_{e0}}{\theta_i}\left(1+\frac{\Psi}{\tau}\right) \\ &+ \frac{\kappa}{\kappa-3/2}\frac{1-\delta}{(1-\Psi/\kappa\tau+2Y/\kappa U\tau)^{\kappa-3/2}}. \end{aligned} \quad (13)$$

III. NUMERICAL EXAMPLES

As a first example of the numerical solution, we choose the following set of input parameters:

$$\begin{aligned} \delta &= 0, \\ U\tau &= 1, \end{aligned} \quad (14)$$

and vary κ. This situation is exactly the same as that considered in Ref. [20]. For the above set of input parameters one can easily see that

$$\begin{aligned} n_i &= n_e, \\ V_i/\theta_i &= -|V_e|/\theta_e, \\ \phi &= 0. \end{aligned} \quad (15)$$

Note that

$$\frac{dY}{dZ} = \frac{B_x}{\sqrt{8\pi n_0\,(\theta_i+\theta_e)}}. \quad (16)$$

Shown in Fig. 1 are normalized B-field and density profiles for $\kappa = 2$, 3, 5, 10, and ∞. The result is identical to that of Ref. [20]. For the present situation, the cross-field drift speeds for ions and electrons are uniform across the current sheet. It is interesting to note that the asymptotic magnetic field strength $dY/dZ|_{Z\to\infty}$ is not unity.

Let us consider the temperature profile [see Eq. (13)]. The result is shown in Fig. 2, which shows that the global temperature profile indefinitely increases as Z^2 increases.

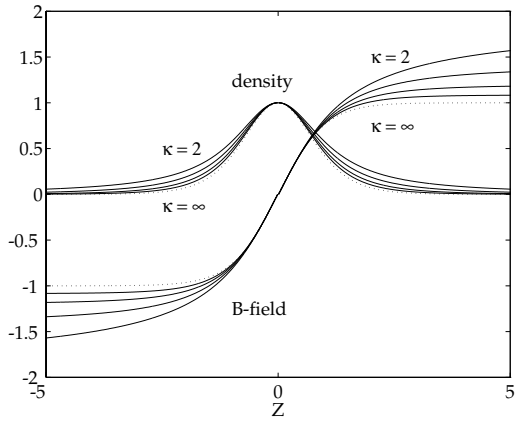

FIG. 1: Normalized B-field and density profiles, dY/dZ and n_j/n_0, respectively, for $\kappa = 2$, 3, 5, 10, and ∞. The case of $\kappa = \infty$ corresponds to the gaussian limit, shown here with the dots.

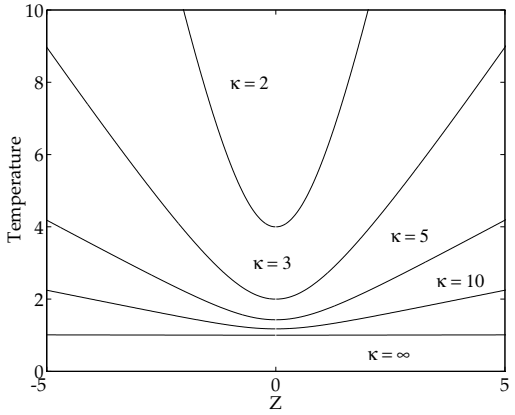

FIG. 2: Global ion temperature profile for $\kappa = 2$, 3, 5, 10, and ∞. The electron temperature profile is the same as that of the ions except that it is scaled with a factor $\tau = \theta_e/\theta_i$.

Clearly such a feature is not physical. To remedy the situation, we next consider a finite background component.

We consider the same set of input parameters as in Fig. 1, and the variation of the background density, δ. For the sake of simplicity, let us focus on the κ value corresponding to $\kappa = 3$. As noted, we still restrict ourselves to the zero electrostatic potential by assuming $U\tau = 1$. For the sake of further simplicity, we also consider that $\theta_{i0} = \theta_{e0} = \theta_i$. Thus, the input parameters are

$$\begin{aligned} \kappa &= 3, \\ U\tau &= 1, \\ \theta_{i0} &= \theta_{e0} = \theta_i. \end{aligned} \tag{17}$$

Shown in Fig. 3 is the global ion temperature profiles for $\delta = 0.2$, 0.4, 0.6, and 0.8. The presence of the background significantly modifies the global temperature profile, as shown by Fig. 3. The temperature profile no longer indefinitely increases as one moves away from the neutral

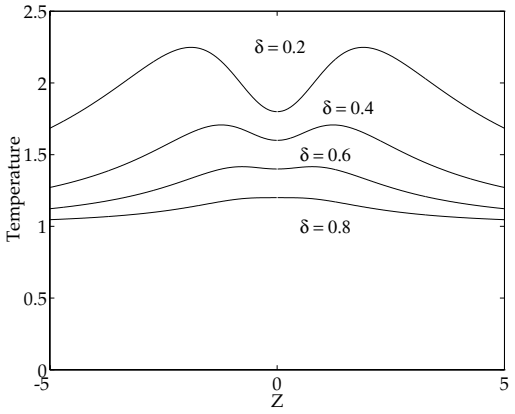

FIG. 3: Global ion temperature profile for $\kappa = 3$ when there is a finite background population, as indicated by finite δ.

sheet, but instead, after the initial rise, it reaches a maximum and then settles down to an asymptotic value. This shows that the presence of the background component is essential from the standpoint of physics when one attempts to model the current sheet with a κ distribution, even though from a purely mathematical point of view, the solution given in Ref. [20] is legitimate.

The present current sheet model is also capable of depicting a slightly charged current sheet, and the embedded current sheet structure. If we allow the condition $U\tau$ to deviate from 1, then the electrostatic potential $\Psi \neq 0$ becomes finite, and the ion and electron drift speed profile no longer takes on the same functional form. In the case of the gaussian current sheet model, a similar discussion was provided in Ref. [21]. The present discussion generalizes Ref. [21] to the case of κ distribution. In the next numerical example, let us consider the following set of input parameters:

$$\begin{aligned} \kappa &= 3, \\ \delta &= 0.5, \\ \theta_{i0} &= \theta_{e0} = \theta_i, \\ \tau &= \frac{\theta_e}{\theta_i} = 0.5, \\ U &= \frac{1}{\tau} + \mathcal{E}, \end{aligned} \tag{18}$$

where $\mathcal{E}$ is unrestricted if it is positive, and $0 < |\mathcal{E}| < 1/\tau$ in the case of the minus value. The case of $\mathcal{E} = 0$ corresponds to the charge-neutral current sheet free of electrostatic potential.

Shown in Fig. 4 are two case of $\mathcal{E}$ corresponding to $\mathcal{E} = -0.5$ and $\mathcal{E} = -1.5$. The negative $\mathcal{E}$ implies embedded electron current layer within thicker ion current, while $\mathcal{E} > 0$ implies the opposite. The embedded electron current sheet structure is not apparently obviously in the case of $\mathcal{E} = -0.5$, but for $\mathcal{E} = -1.5$ (note that $|\mathcal{E}|$ cannot exceed $1/\tau = 2$) the narrow electron current layer

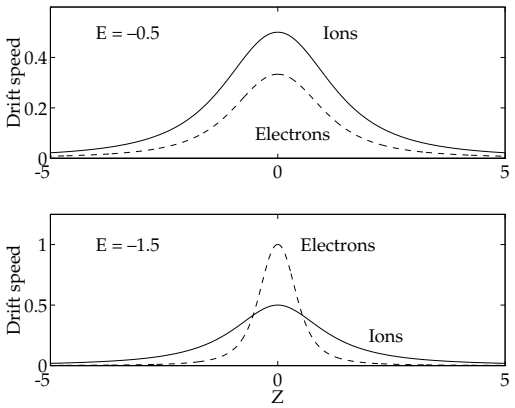

FIG. 4: Embedded current sheet for $\mathcal{E} = -0.5$ (top) and $\mathcal{E} = -1.5$ (bottom). In the bottom panel, the embedded electron current layer within the thicker ion current is plainly obvious.

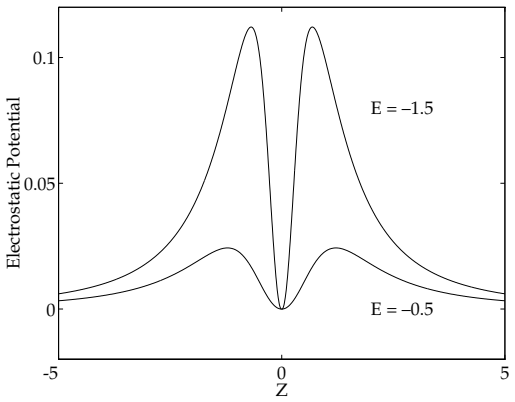

FIG. 5: Electrostatic potentials across the current sheet for $\mathcal{E} = -0.5$ and $\mathcal{E} = -1.5$.

embedded within the thicker ion current layer is plainly seen.

The discrepancy in the electron and ion current profiles is maintained by an equilibrium electrostatic potential difference across the current sheet. Figure 5 plots the corresponding electrostatic potential Ψ for the two cases $\mathcal{E} = -0.5$ and $\mathcal{E} = -1.5$. For positive $\mathcal{E}$, the sign of the potential Ψ reverses (see Ref. [21] for more in-depth discussion in the case of gaussian current sheet). In the slightly-charged current sheet of the type presently discussed, the particles will experience $\mathbf{E} \times \mathbf{B}$ force in addition to the diamagnetic drifts. The additional cross-field drifts of the particles may affect the stability of the current sheet in a significant manner. For instance, Refs. [23, 24] argue that an electromagnetic cross-field current instability driven by the combined $\mathbf{E} \times \mathbf{B}$ and the diamagnetic drifts might be highly relevant for the reconnection onset.

Before we close, let us return to the issue of global temperature profile. Figure 6 plots the ion and electron temperature profiles across the current sheet for $\mathcal{E} = -0.5$ and $\mathcal{E} = -1.5$. As one can appreciate, the global temperature profiles associated with the present charged current sheet display physically proper characteristics in that there is no divergence and that their asymptotic values are finite.

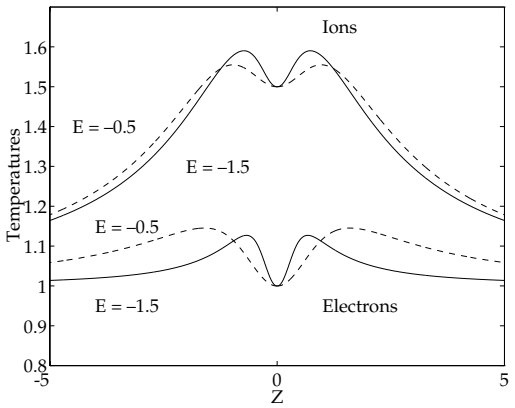

FIG. 6: Ion and electron temperature profiles across the current sheet for $\mathcal{E} = -0.5$ and $\mathcal{E} = -1.5$.

IV. CONCLUSIONS

In the present paper we (re)derived current sheet equilibrium solutions on the basis of the so-called κ distribution functions for the particles. The purpose of the present paper was to remedy a shortcoming in a recent paper by Fu and Hau [20], where the authors formulated the equilibrium current sheet model with the κ distribution for the first time. Although mathematically correct, their model contains a peculiarly unphysical feature in that the global temperature profile diverges in the asymptotic regime. The present paper has shown that such an unphysical characteristics can be rectified if one assumes a finite stationary background population of the particles. We further extended the analysis to allow the solution to possess a feature in which the electron current is embedded within a thicker ion current layer (or *vice versa*), and where there exists a weak electrostatic potential drop across the current sheet. The potential significance of the embedded/slightly-charged current sheet on the stability property was also discussed.

The present research was supported by NSF Grant ATM 0535824 to the University of Maryland, and by NASA Grant NNG04G128G to The Johns Hopkins University Applied Physics Laboratory.

* Email:yoonp@ipst.umd.edu
† Email:tony.lui@jhuapl.edu
‡ Email:Rob.Sheldon@msfc.nasa.gov

[1] G. K. Parks, *Physics of Space Plasmas: An introduction*, 2nd Ed. (Addison-Wesley, Redwood City, 2004).
[2] M. G. Kivelson, J. Warnecke, L. Bennett, S. Joy, K. K. Khurana, J. A. Linker, C. T. Russell, R. J. Walker, C. Polanskey, J. Geophys. Res. **103**, 19963 (1998).
[3] D. Biskamp, *Magnetic reconnection in plasmas* (Cambridge University Press, Cambridge, 2000).
[4] A. T. Y. Lui, J. Geophys. Res. **101**, 13067 (1996).
[5] P. H. Yoon and A. T. Y. Lui, Phys. Fluids B **5**, 836 (1993).
[6] P. H. Yoon, A. T. Y., Lui, and M. I. Sitnov, Phys. Plasmas **9**, 1526 (2002).
[7] W. Daughton, G. Lapenta, and P. Rici, Phys. Rev. Lett. **93**, 105004 (2004).
[8] P. Rici, J. U. Brackbill, W. Daughton, G. Lapenta, Phys. Plasmas **11**, 4489 (2004).
[9] G. Consolini, M. Kretzschmar, A. T. Y. Lui, G. Zimbardo, W. M. Macek, J. Geophys. Res. **110**, A07202 (2005).
[10] E. Camporeale and G. Lapenta, J. Geophys. Res. **110**, A07206 (2005).
[11] S. P. Christon, D. J. Williams, D. G. Mitchell, L. A. Frank, and C. Y. Huang, J. Geophys. Res. **94**, 13409 (1989).
[12] E. G. Harris, Nuovo Cimento **23**, 115 (1961).
[13] V. M. Vasyliunas, J. Geophys. Res. **73**, 2839 (1968).
[14] C. Tsallis, J. Stat. Phys. **52**, 479 (1988).
[15] M. P. Leubner, Astrophys. Space Sci. **282**, 573 (2002).
[16] M. P. Leubner, Astrophys. J. **604**, 469 (2004).
[17] M. P. Leubner, Phys. Plasmas **11**, 1308 (2004).
[18] R. A. Treumann, Phys. Scr. **59**, 19 (1999).
[19] R. A. Treumann, Phys. Scr. **59**, 204 (1999).
[20] W.-Z. Fu and L.-N. Hau, Phys. Plasmas **12**, 070701 (2005).
[21] P. H. Yoon and A. T. Y. Lui, J. Geophys. Res. **109**, A11213 (2004).
[22] A. D. Polyanin and V. F. Zaitsev, *Handbook of Exact Solutions for Ordinary Differential Equations*, 2nd Ed., (CRC Press, New York, 2003), p. 307.
[23] R. Kulsrud, H. Ji, W. Fox, and M. Yamada, Phys. Plasmas **12**, 082301 (2005).
[24] H. Ji, R. Kulsrud, W. Fox, and M. Yamada, J. Geophys. Res. **110**, A08212 (2005).